

Multilevel quantum thermodynamic swap engines

Massimiliano F. Sacchi^{1,2,*}

¹*CNR - Istituto di Fotonica e Nanotecnologie, Piazza Leonardo da Vinci 32, I-20133, Milano, Italy,*
²*QUIT Group, Dipartimento di Fisica, Università di Pavia, via A. Bassi 6, I-27100 Pavia, Italy.*

We study energetic exchanges and fluctuations in two-stroke quantum thermodynamic engines where the working fluid is represented by two multilevel quantum systems, i.e. qudits, the heat flow is allowed by relaxation with two thermal reservoirs at different temperatures, and the work exchange is operated by a partial-swap unitary interaction. We identify three regimes of operation (heat engine, refrigerator, and thermal accelerator), present the thermodynamic uncertainty relations between the entropy production and the signal-to-noise ratio of work and heat, and derive the full joint probability of the stochastic work and heat. Our results bridge the gap between two-qubit and two-mode bosonic swap engines, and show which properties are maintained (e.g., a non fluctuating Otto efficiency) and which are lost for increasing dimension (e.g., small violations of the standard thermodynamic uncertainty relations or the possibility of beating the Curzon-Ahlborn efficiency).

arXiv:2106.15897v2 [quant-ph] 14 Jul 2021

* msacchi@unipv.it

I. INTRODUCTION

A growing interest has been recently devoted to thermodynamic engines where the working systems are operated at the nanoscale [1–3], from electronic devices [4, 5] to biological or chemical systems [6–8]. Differently from the usual scenery of macroscopic thermodynamics, when the working substances are elementary and small enough and generally when the discrete nature of the energy spectrum is relevant, the fluctuations of the thermodynamical variables become very important, and the theoretical approach in terms of stochastic thermodynamics [9–11] turns out to be very useful to address the problem of quantifying the efficiency along with the stability and reliability of quantum thermodynamic engines.

In fact, fluctuation relations [10–29] pose rigid constraints on the statistics of heat, work and entropy production in terms of the symmetries of the elemental microscopic dynamics. More recently, so-called thermodynamic uncertainty relations (TUR) have been developed [30–50], where the signal-to-noise ratio of observed work and heat has been related to the entropy production. For example, these TURs balance the tradeoff between entropy production and fluctuations of output power, namely the precision of a heat engine, such that working systems operating at vanishing entropy production entail a divergence in the relative output power fluctuations. Fluctuation relations and TURs have been independently developed, but lately they have been connected within various approaches and operational assumptions [36, 51–59], suited also to the analysis of quantum thermodynamic stroke engines [53, 60].

One of the most studied quantum thermodynamic engines is based on the Otto cycle [60–71], with possible implementations by different physical systems as working fluid, e.g. ion traps, Cooper-pair boxes, or quantized modes of the radiation field. The advantage of stroke Otto engines is that a deep study is amenable, since heat and work strokes are clearly separated: in a part of the dynamics, the systems are coupled to thermal reservoirs and are allowed to relax with fixed Hamiltonian by heat exchange, while in a different part they are isolated from the baths and work is externally supplied or extracted by driven Hamiltonian. In fact, a thorough derivation of the full stochastic heat and work distribution can be accomplished when the working strokes are operated by a partial-swap unitary interaction, when the working fluid is represented by two bosonic modes or two qubits [60].

Building on the approach of Ref. [60], in this paper we study a two-stroke thermodynamic engine where the working fluid is abstractly given by two multilevel quantum systems (i.e. qudits), each with equally-spaced energy levels. These are alternately coupled to their own thermal bath at different temperatures allowing heat exchange, whereas the working stroke is implemented by a unitary interaction with tunable partial swap in order to extract or supply work. In the situation of perfect swap operation, this model interpolates the case of two qubits with that of two harmonic oscillators under 50/50 frequency conversion [60], and may find application with different high-dimensional quantum systems, as Rydberg atoms [72], polar molecules [73], trapped ions [74], NMR systems [75], cold atomic ensembles [76, 77], and discretized degrees of freedom of photons [78].

By the joint estimation of work and heat via a two-point-measurement scheme [11, 26, 79, 80], we obtain the characteristic function that provides all moments of work and heat. Three regimes of operation are identified, where the periodic protocol works as a heat engine, a refrigerator, or a thermal accelerator. The model is shown to achieve the Otto efficiency, independently of the dimension, the temperature of the reservoirs, and the coupling parameter. We present an exact relation between the signal-to-noise ratio of work and heat and the average entropy production of the engine, thus linking together average extracted work, fluctuations, and entropy production. From these relations we derive thermodynamic uncertainty relations that are satisfied in all the regimes of operations and for any dimension. Similarly to the case of two-qubit stroke engines [53, 60], a small violation of the standard TUR is observed, which, however, is rapidly washed out for increasing dimension of the working qudits or for decreasing coupling strength. A bound of the efficiency in terms of the first two moments of the work distribution is also obtained. Finally, we provide the full joint probability of the discrete stochastic work and heat in closed form, which allows to explicitly verify a detailed fluctuation theorem. We conclude the paper with a preliminary analysis of the finite-time cycle, i.e. by considering partial thermalization strokes, and study the resulting output power in the case of perfect-swap unitary interaction. In this case we show the possibility of beating the Curzon-Ahlborn efficiency [81–83], which however is reduced for increasing dimension.

II. A TWO-QUDIT SWAP ENGINE

Throughout the paper we fix natural units for both Planck and Boltzmann constants, namely $\hbar = k_B = 1$. The thermodynamic engine under investigation is based on a working fluid given by a couple of qudits A and B , i.e. two d -level quantum systems, each one with equally-spaced energy levels. We can write their free Hamiltonian as

$$H_C = \omega_C \sum_{n=0}^{d-1} n |n\rangle, \quad (1)$$

with $C = A, B$. Initially, the two qudits are in thermal equilibrium with their own ideal bath at temperature T_A and T_B , respectively, and we fix $T_A > T_B$. Hence, the initial state is described by the tensor product of Gibbs thermal states, i.e.

$$\rho_0 = \frac{e^{-\beta_A H_A}}{Z_A} \otimes \frac{e^{-\beta_B H_B}}{Z_B}, \quad (2)$$

with $\beta_X = 1/T_X$ and $Z_X = \text{Tr}[e^{-\beta_X H_X}] = \frac{1 - e^{-d\beta_X \omega_X}}{1 - e^{-\beta_X \omega_X}}$. The two qudits are then isolated from their thermal baths and are allowed to interact in a time window $[0, \tau_w]$ via the time-dependent interaction

$$H(t) = \kappa e^{-i(H_A + H_B)t} E e^{i(H_A + H_B)t}, \quad (3)$$

where κ is a real coupling parameter and E denotes the swap operator, which acts on two-qudit states as $E|\psi\rangle \otimes |\varphi\rangle = |\varphi\rangle \otimes |\psi\rangle$. In the interaction picture where

$$\rho_I(t) = U_0^\dagger(t) \rho(t) U_0(t), \quad (4)$$

with $U_0(t) = \exp[-i(H_A + H_B)t]$, the interaction Hamiltonian is clearly

$$H_I(t) \equiv H_I = H(0) = \kappa E, \quad (5)$$

and hence one has $\rho_I(t) = e^{-iH_I t} \rho_I(0) e^{iH_I t}$. Going back to the Schrödinger picture we obtain the evolution

$$\rho(t) \equiv U(t) \rho(0) U^\dagger(t) = U_0(t) e^{-iH_I t} \rho(0) e^{iH_I t} U_0^\dagger(t). \quad (6)$$

Since $E^2 = I$ we can also write

$$V_\theta \equiv e^{-iH_I \tau_w} = \cos \theta I - i \sin \theta E, \quad (7)$$

with $\theta = \kappa \tau_w$, and hence $U(\tau_w) = U_0(\tau_w) V_\theta$.

After the interaction the two qudits are reset to their equilibrium state of Eq. (2) via complete thermalization by their respective baths. The procedure can be sequentially repeated and leads to a two-stroke engine. For each cycle the energy change in qudit A corresponds to the heat Q_H released by the hot bath, i.e. $Q_H = -\Delta E_A$, and similarly for qudit B we have $Q_C = -\Delta E_B$, corresponding to the heat dumped into the cold reservoir (heat is positive when flowing out of a reservoir). The work W is supplied ($W > 0$) or extracted ($W < 0$) during the unitary interaction, and the first law $W = -Q_H - Q_C = \Delta E_A + \Delta E_B$ holds. The entropy production per cycle is then given by $\Sigma = -\beta_A Q_H - \beta_B Q_C = (\beta_B - \beta_A) Q_H + \beta_B W$.

We characterize the engine by the independent variables W and Q_H , and consider the characteristic function $\chi(\lambda, \mu)$, where λ and μ denote the counting parameters for work and heat, so that all moments can be recovered as

$$\langle W^l Q_H^s \rangle = (-i)^{l+s} \left. \frac{\partial^{l+s} \chi(\lambda, \mu)}{\partial \lambda^l \partial \mu^s} \right|_{\lambda=\mu=0}. \quad (8)$$

By adopting the two-point measurement protocol [11, 26, 79, 80] typically considered in the derivation of Jarzynski equality [84] to jointly estimate W and Q_H , in the present scenario the characteristic function can be written as

$$\chi(\lambda, \mu) = \text{Tr}[U^\dagger(\tau_w) (e^{i(\lambda-\mu)H_A} \otimes e^{i\lambda H_B}) U(\tau_w) (e^{-i(\lambda-\mu)H_A} \otimes e^{-i\lambda H_B}) \rho_0]. \quad (9)$$

Equation (9) can be obtained along similar lines as in Refs. [24, 26], and a brief derivation is given in Appendix A for the sake of the reader. The explicit evaluation of the characteristic function is presented in Appendix B with the following result

$$\chi(\lambda, \mu) = \cos^2 \theta + \sin^2 \theta \frac{\sinh\left(\frac{\beta_A \omega_A}{2}\right) \sinh\left(\frac{\beta_B \omega_B}{2}\right) \sinh\left[\frac{d}{2}(\beta_A \omega_A + i\xi)\right] \sinh\left[\frac{d}{2}(\beta_B \omega_B - i\xi)\right]}{\sinh\left(\frac{d\beta_A \omega_A}{2}\right) \sinh\left(\frac{d\beta_B \omega_B}{2}\right) \sinh\left[\frac{1}{2}(\beta_A \omega_A + i\xi)\right] \sinh\left[\frac{1}{2}(\beta_B \omega_B - i\xi)\right]}, \quad (10)$$

where $\xi = (\omega_A - \omega_B)\lambda - \omega_A \mu$. We note the identity $\chi[i\beta_B, i(\beta_B - \beta_A)] = 1$, corresponding to the standard fluctuation theorem $\langle e^{-\Sigma} \rangle = 1$. In fact, the stronger relation $\chi[i\beta_B - \lambda, i(\beta_B - \beta_A) - \mu] = \chi(\lambda, \mu)$ holds [85], which is equivalent to the detailed fluctuation theorem [22, 24, 25, 27]

$$\frac{p(W, Q_H)}{p(-W, -Q_H)} = e^{(\beta_B - \beta_A) Q_H + \beta_B W} = e^\Sigma. \quad (11)$$

We notice that for $\theta = \pi/2$ the unitary $V_{\pi/2}$ performs a swap gate which exchanges the states of the two quantum systems. In this situation, in the limit $d \rightarrow \infty$ the two-qudit model recovers the two-mode bosonic Otto engine of Ref. [60] under 50/50 frequency conversion [86].

Since $\chi(\lambda, \mu)$ is a function of the single variable ξ , one has $\partial_\mu \chi = \frac{\omega_A}{\omega_B - \omega_A} \partial_\lambda \chi$. Hence, from Eq. (8) one obtains the symmetry relations

$$\langle W^l Q_H^s \rangle = \left(\frac{\omega_A}{\omega_B - \omega_A} \right)^s \langle W^{l+s} \rangle, \quad (12)$$

and, from the first law, $\langle Q_C^l \rangle = (-\omega_B/\omega_A)^l \langle Q_H^l \rangle$. It follows that the average entropy production per cycle is given by

$$\langle \Sigma \rangle \equiv -\beta_A \langle Q_H \rangle - \beta_B \langle Q_C \rangle = \frac{\beta_A \omega_A - \beta_B \omega_B}{\omega_A - \omega_B} \langle W \rangle. \quad (13)$$

From the characteristic function we can now evaluate the average work per cycle, which is given by

$$\langle W \rangle = \frac{\sin^2 \theta}{2} (\omega_B - \omega_A) \{ \coth(\beta_A \omega_A / 2) - d \coth(d \beta_A \omega_A / 2) - [\coth(\beta_B \omega_B / 2) - d \coth(d \beta_B \omega_B / 2)] \}. \quad (14)$$

Correspondingly, from Eq. (12), the heat exchanged with the hot reservoir is $\langle Q_H \rangle = \frac{\omega_A}{\omega_B - \omega_A} \langle W \rangle$. We note that for any positive integer d the function $\coth(x/2) - d \coth(dx/2)$ is monotonic decreasing versus x . Hence, we can identify three regimes of operation of the quantum thermodynamic machine, namely

- a) $1 < \frac{\omega_A}{\omega_B} < \frac{T_A}{T_B}$ heat engine,
- b) $\frac{\omega_A}{\omega_B} > \frac{T_A}{T_B}$ refrigerator,
- c) $\frac{\omega_A}{\omega_B} < 1$ thermal accelerator,

where we have respectively

- a) $\langle W \rangle < 0, \quad \langle Q_H \rangle > 0, \quad \langle Q_C \rangle < 0;$
- b) $\langle W \rangle > 0, \quad \langle Q_H \rangle < 0, \quad \langle Q_C \rangle > 0;$
- c) $\langle W \rangle > 0, \quad \langle Q_H \rangle > 0, \quad \langle Q_C \rangle < 0.$

In Fig. 1 we plot the average work, heat and entropy production for dimensions $d = 2, 4$, and 8 , for parameters $T_A = 1, T_B = 2, \theta = \pi/2, \omega_A = 1$ versus ω_B/ω_A .

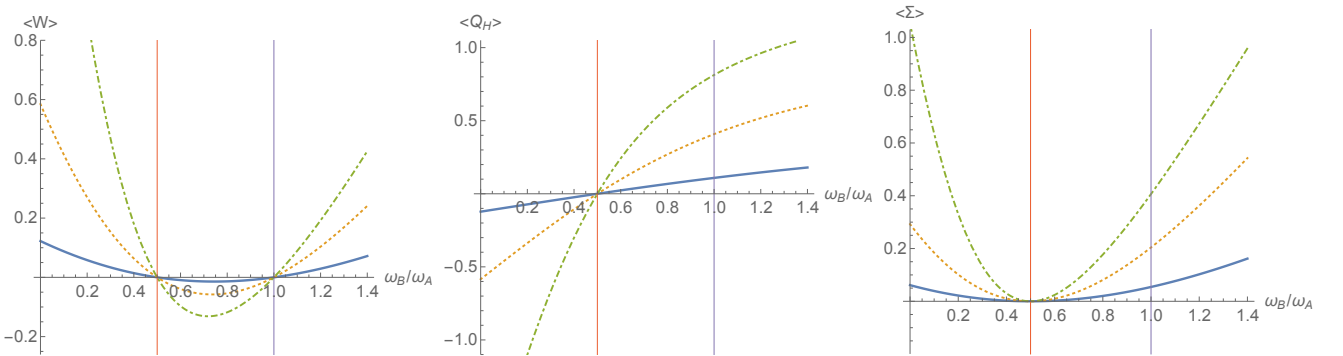


Figure 1. Average work (left), heat (center) and entropy production (right) for parameters $T_A = 2, T_B = 1, \theta = \pi/2, \omega_A = 1$ versus ω_B/ω_A , for dimension $d = 2$ (solid line), $d = 4$ (dotted), and $d = 8$ (dot-dashed). The three regimes of operation correspond to $\omega_B/\omega_A < \frac{1}{2}$ (refrigerator), $\frac{1}{2} < \omega_B/\omega_A < 1$ (heat engine), and $\omega_B/\omega_A > 1$ (thermal accelerator).

As expected, from Eq. (13) it follows that the entropy production $\langle \Sigma \rangle$ is always positive. Upon defining the mean occupation number

$$N_X = \text{Tr} \left[\frac{e^{-\beta_X H_X}}{Z_X} \frac{H_X}{\omega_X} \right] = \frac{1}{2} [d - 1 + \coth(\beta_X \omega_X / 2) - d \coth(d \beta_X \omega_X / 2)] \equiv g(\beta_X \omega_X), \quad (15)$$

we can also rewrite concisely

$$\langle W \rangle = \sin^2 \theta (\omega_B - \omega_A) (N_A - N_B) . \quad (16)$$

The efficiency η of the heat engine is given by $\eta = \frac{\langle -W \rangle}{\langle Q_H \rangle} = 1 - \frac{\omega_B}{\omega_A} \leq 1 - \frac{T_B}{T_A} \equiv \eta_C$, corresponding to the Otto cycle efficiency. The Carnot efficiency η_C is achieved only for $\omega_A/\omega_B = T_A/T_B$ (i.e., with zero output work). Analogously, the coefficient of performance for the refrigerator is given by $\zeta = \frac{\langle Q_C \rangle}{\langle W \rangle} = \frac{\omega_B}{\omega_A - \omega_B} \leq \frac{T_B}{T_A - T_B} = \zeta_C$. Notice that both η and ζ are independent of the coupling strength θ , the temperature of the reservoirs, and the dimension d .

The present model shares some similarities with those studied in Refs. [70, 71], where the same Otto efficiency is achieved. In particular, in Ref. [71] the interaction between the working systems is modeled by a beamsplitter-like Hamiltonian, and the same regimes of operation are obtained. In fact, in both models the total excitation number of the systems is preserved by the working interaction. Here, these feature is easily seen by the symmetry relation

$$[H_I(t), H_A/\omega_A + H_B/\omega_B] = 0 . \quad (17)$$

We can find (numerically) the efficiency η_m at maximum work per cycle. The result is plotted in Fig. 2, for different values of the dimension d : one finds that η_m is *larger* than the Curzon-Ahlborn efficiency $\eta_{CA} = 1 - \sqrt{T_B/T_A}$, i.e. the efficiency of the endoreversible Carnot cycle at maximum power [81–83] and rapidly converges to η_{CA} for increasing values of the dimension d (see Appendix C for the limiting case $d \rightarrow \infty$).

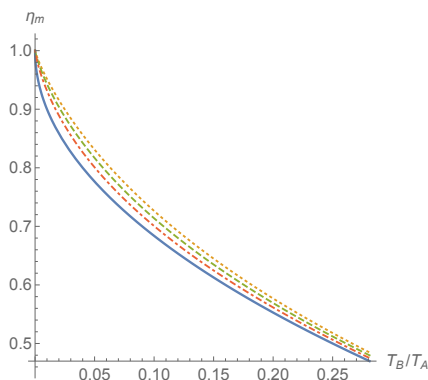


Figure 2. Efficiency at maximum work η_m versus the ratio T_B/T_A for dimension $d = 2$ (dotted), 4 (dashed), and 8 (dot-dashed), along with the Curzon-Ahlborn curve $\eta_{CA} = 1 - \sqrt{T_B/T_A}$ in solid line.

By the identity $\frac{\beta_A \omega_A - \beta_B \omega_B}{\omega_A - \omega_B} = -\frac{1}{T_B} \left(\frac{\eta_C}{\eta} - 1 \right)$, one obtains the relation

$$\langle \Sigma \rangle = \frac{\langle -W \rangle}{T_B} \left(\frac{\eta_C}{\eta} - 1 \right) \quad (18)$$

between average extracted work, entropy production and efficiency of the heat engine. Analogously, one has $\langle \Sigma \rangle = \frac{\langle Q_C \rangle}{T_A} \left(\frac{1}{\zeta} - \frac{1}{\zeta_C} \right)$ for the refrigerator. Notice that these relations hold also for the two-qubit and two-mode bosonic Otto engines [60].

III. THERMODYNAMIC UNCERTAINTY RELATIONS AND PROBABILITY OF STOCHASTIC WORK AND HEAT

The second moments of work $\langle W^2 \rangle$, heat $\langle Q_H^2 \rangle$, and the correlation $\langle W Q_H \rangle$ can be obtained through Eqs. (8) and (10) by lengthy but straightforward calculation, and one has

$$\begin{aligned} \langle W^2 \rangle = & \frac{\sin^2 \theta}{2} (\omega_B - \omega_A)^2 \{ d^2 - 1 + \coth^2(\beta_A \omega_A/2) + \coth^2(\beta_B \omega_B/2) - \coth(\beta_A \omega_A/2) \coth(\beta_B \omega_B/2) \\ & - d[\coth(\beta_A \omega_A/2) - \coth(\beta_B \omega_B/2)][\coth(d\beta_A \omega_A/2) - \coth(d\beta_B \omega_B/2)] \\ & - d^2 \coth(d\beta_A \omega_A/2) \coth(d\beta_B \omega_B/2) \} , \end{aligned} \quad (19)$$

$$\langle Q_H^2 \rangle = \frac{\omega_A^2}{(\omega_B - \omega_A)^2} \langle W^2 \rangle , \quad (20)$$

$$\langle W Q_H \rangle = \frac{\omega_A}{\omega_B - \omega_A} \langle W^2 \rangle . \quad (21)$$

From the above equations, along with Eq. (13), we find an exact identity relating the inverse signal-to noise ratios and the entropy production, namely

$$\frac{\text{var}(W)}{\langle W \rangle^2} = \frac{\text{var}(Q)}{\langle Q_H \rangle^2} = \frac{\text{cov}(W, Q_H)}{\langle W \rangle \langle Q_H \rangle} = \frac{(\beta_B \omega_B - \beta_A \omega_A) f(\beta_A \omega_A, \beta_B \omega_B, d)}{\langle \Sigma \rangle} - 1, \quad (22)$$

with

$$\begin{aligned} f(x, y, d) = & \{d^2 - 1 + \coth^2(x/2) + \coth^2(y/2) - \coth(x/2) \coth(y/2) \\ & - d[\coth(x/2) - \coth(y/2)][\coth(dx/2) - \coth(dy/2)] - d^2 \coth(dx/2) \coth(dy/2)\} \\ & \times \{\coth(x/2) - \coth(y/2) - d[\coth(dx/2) - \coth(dy/2)]\}^{-1}. \end{aligned} \quad (23)$$

We note that the only dependence on the coupling parameter θ comes for the inverse of the average entropy production $\langle \Sigma \rangle$. Hence, the above ratios are minimized versus θ for $\theta = \frac{\pi}{2}$, for which also the entropy production achieves the maximum. Then, the reduction of the noise-to-signal ratio associated to work extraction (or cooling performance) comes at a price of increased entropy production. We observe that for $\theta = \pi/2$ the unitary stroke transforms the initial bi-thermal state (2) with inverse temperatures β_A and β_B into a bi-thermal state with final inverse temperatures $\beta_B \omega_B / \omega_A$ and $\beta_A \omega_A / \omega_B$ without leaving final correlations between the two qudits. On the other hand, operating at zero entropy production (i.e., for $\beta_A \omega_A \rightarrow \beta_B \omega_B$, thus approaching the Carnot efficiency) will induce a divergence in Eq. (22).

For the heat-engine regime $\beta_A \omega_A < \beta_B \omega_B$ and fixed values of d and θ , numerical inspection shows that for assigned value of $\beta_A \omega_A$ (of $\beta_B \omega_B$) the ratio $\frac{\text{var}(W)}{\langle W \rangle^2}$ is minimized for $\beta_B \omega_B \rightarrow \infty$ (for $\beta_A \omega_A \rightarrow 0$), and the ultimate minimization is given by

$$\frac{\text{var}(W)}{\langle W \rangle^2} = \frac{d + 1 + 3(d-1) \cos^2 \theta}{3(d-1) \sin^2 \theta}, \quad (24)$$

achieved for $\beta_A \omega_A \rightarrow 0$ and $\beta_B \omega_B \rightarrow \infty$.

Note that for both the heat engine and the refrigerator the sign of $\text{cov}(W, Q_H)$ is negative, whereas for the thermal accelerator where external work is supplied to increase the heat flow from hot to cold reservoir the covariance is positive.

For $d = 2$, since the function g in Eq. (15) is easily inverted, namely $\beta_X \omega_X = \ln \frac{1-N_X}{N_X}$, Eq. (19) can be rewritten as

$$\langle W^2 \rangle = \sin^2 \theta (\omega_B - \omega_A)^2 (N_A + N_B - 2N_A N_B), \quad (25)$$

thus recovering the result for qubits [60]. Also Eq. (23) simplifies as

$$f(x, y, 2) = \coth[(y-x)/2]. \quad (26)$$

From numerical evidence one has $(y-x)f(x, y, d) \geq 2$, with equality in the limit $x \rightarrow y$, and hence the following TUR is obtained

$$\frac{\text{var}(W)}{\langle W \rangle^2} \geq \frac{2}{\langle \Sigma \rangle} - 1, \quad (27)$$

which holds for all parameters and any dimension d . As in the two-qubit case, the presence of the -1 term implies that the standard TUR $\frac{\text{var}(W)}{\langle W \rangle^2} \geq \frac{2}{\langle \Sigma \rangle}$ can be slightly violated [53, 60]. Remarkably, a similar small violation has been recently reported in Ref. [87] for a different model of thermal machine (i.e. a two-qubit steady-state and autonomous engine), where also a stronger violation is found for a three-qubit model.

In Fig. 3 we report the signal-to-noise ratio $\langle W \rangle^2 / \text{var}(W)$ along with the function $\langle \Sigma \rangle / 2$ for the cases $d = 2$ and $d = 8$ with $\theta = \pi/2$. We generally observe that the region of parameter space for a violation of the standard TUR is shrunk for increasing values of the dimension d . This is more apparent in Fig. 4, where the product $\text{var}(W) \langle \Sigma \rangle / \langle W \rangle^2$ is reported versus $\beta_B \omega_B$ for fixed $\beta_A \omega_A = 0.1$, coupling $\theta = \pi/2$ and dimension $d = 2, 4$, and 6. Indeed, we recall that for the two-mode bosonic engine the standard TUR is never violated, since $\frac{\text{var}(W)}{\langle W \rangle^2} \geq \frac{2}{\langle \Sigma \rangle} + 1$ holds [60]. A similar shrinking effect is observed also for decreasing values of the coupling θ at fixed dimension d , along with a rapid decrease of the strength of the violations, as shown for example in Fig. 5 for the case $d = 2$ with coupling values $\theta = \pi/2, 5\pi/12$, and $\pi/3$. We report that the strongest violation of the standard TUR is numerically obtained for $d = 2$, $\theta = \pi/2$, $\beta_A \omega_A \rightarrow 0$, and $\beta_B \omega_B \simeq 2.010$, for which $\text{var}(W) \langle \Sigma \rangle / \langle W \rangle^2 \simeq 1.864$.

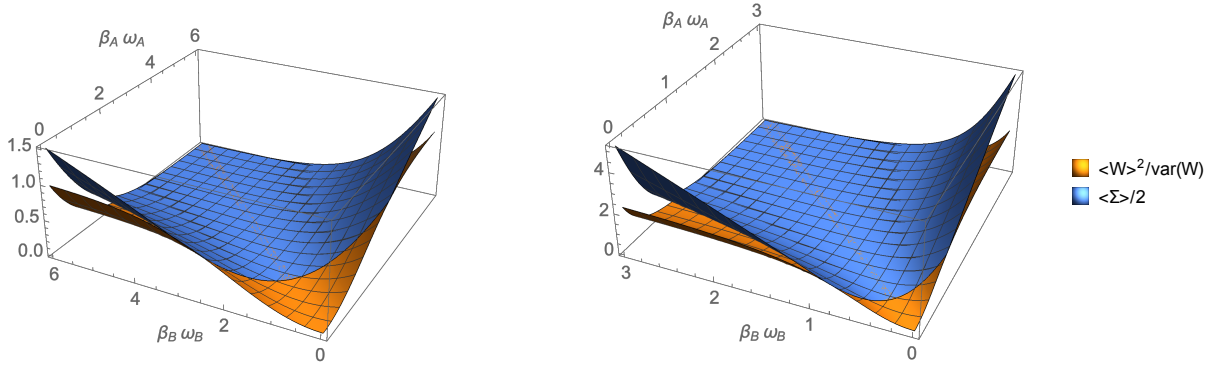


Figure 3. Plot of the signal-to-noise ratio of work $\langle W \rangle^2 / \text{var}(W)$ and scaled entropy production $\langle \Sigma \rangle / 2$ with coupling $\theta = \pi/2$ for dimension $d = 2$ (left) and $d = 8$ (right) as a function of parameters $\beta_A \omega_A$ and $\beta_B \omega_B$. The region of parameter space where the standard TUR is violated is shrunk for increasing dimension of the working systems.

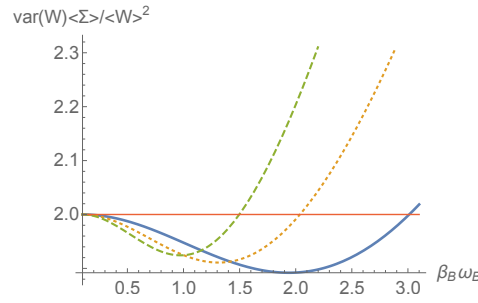


Figure 4. Ratio $\text{var}(W) \langle \Sigma \rangle / \langle W \rangle^2$ versus $\beta_B \omega_B$ with $\beta_A \omega_A = 0.1$, $\theta = \pi/2$, and dimension $d = 2$ (solid line), 3 (dotted), and 4 (dashed).

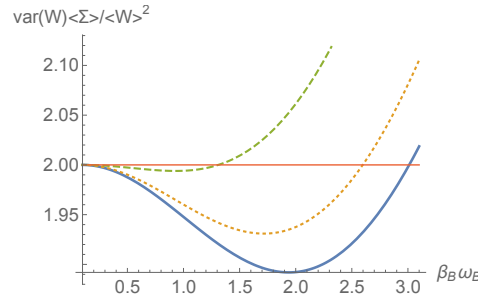


Figure 5. Ratio $\text{var}(W) \langle \Sigma \rangle / \langle W \rangle^2$ versus $\beta_B \omega_B$ with $\beta_A \omega_A = 0.1$, $d = 2$, and coupling strength $\theta = \pi/2$ (solid line), $5\pi/12$ (dotted), and $\pi/3$ (dashed).

From Eq. (18) and the bound $\frac{\langle W^2 \rangle}{\langle W \rangle^2} \geq \frac{2}{\langle \Sigma \rangle}$ equivalent to Eq. (27), we can obtain the following relation between the average extracted work, second moment and efficiency

$$\langle -W \rangle \leq \frac{\langle W^2 \rangle}{2T_B} \left(\frac{\eta_C}{\eta} - 1 \right), \quad (28)$$

which can also be written as a bound on the efficiency, namely

$$\eta \leq \frac{\eta_C}{1 + 2T_B \langle -W \rangle / \langle W^2 \rangle}. \quad (29)$$

Hence, in order to increase the efficiency, one must either reduce the output work or increase the second moment of work distribution, thus undermining the engine reliability. For the two-mode bosonic Otto engine analogous equations as (28) and (29) hold [60], when replacing $\langle W^2 \rangle$ with $\text{var}(W)$.

Since the characteristic function is periodic in λ and μ with period $\frac{2\pi}{|\omega_A - \omega_B|}$ and $\frac{2\pi}{\omega_A}$ the joint probability $p(W, Q_H)$ of the stochastic work and heat is discrete, with W and Q_H as integer multiples of $\omega_A - \omega_B$ and ω_A , respectively. Then one has

$$p[W = m(\omega_A - \omega_B), Q_H = n\omega_A] = \frac{\omega_A |\omega_A - \omega_B|}{(2\pi)^2} \int_{-\frac{\pi}{|\omega_A - \omega_B|}}^{\frac{\pi}{|\omega_A - \omega_B|}} d\lambda \int_{-\frac{\pi}{\omega_A}}^{\frac{\pi}{\omega_A}} d\mu \chi(\lambda, \mu) e^{-im(\omega_A - \omega_B)\lambda - in\omega_A\mu}. \quad (30)$$

Since $\chi(\lambda, \mu)$ is a function of the single variable $\xi = (\omega_A - \omega_B)\lambda - \omega_A\mu$, namely $\chi(\lambda, \mu) = \chi\left(0, \mu - \frac{(\omega_A - \omega_B)\lambda}{\omega_A}\right)$, by the change of variables $\mu \rightarrow \omega_A\mu - (\omega_A - \omega_B)\lambda$ and $\lambda \rightarrow (\omega_A - \omega_B)\lambda$ in Eq. (30) we obtain

$$\begin{aligned} p[W = m(\omega_A - \omega_B), Q_H = n\omega_A] &= \frac{1}{(2\pi)^2} \int_{-\pi}^{\pi} d\lambda \int_{-\pi-\lambda}^{\pi-\lambda} d\mu \chi\left(0, \frac{\mu}{\omega_A}\right) e^{-i(n+m)\lambda - in\mu} \\ &= \int_0^{2\pi} \frac{d\mu}{2\pi} \chi\left(0, \frac{\mu}{\omega_A}\right) e^{-in\mu} \int_{-\pi}^{\pi} \frac{d\lambda}{2\pi} e^{-i(n+m)\lambda} = \delta_{m,-n} \int_0^{2\pi} \frac{d\mu}{2\pi} \chi\left(0, \frac{\mu}{\omega_A}\right) e^{-in\mu}. \end{aligned} \quad (31)$$

This means that the stochastic work and heat are perfectly correlated, i.e.

$$p[W = m(\omega_A - \omega_B), Q_H = n\omega_A] = p[W = m(\omega_A - \omega_B)]\delta_{n,-m} = p[Q_H = n\omega_A]\delta_{m,-n}. \quad (32)$$

This feature is due to the symmetry (17) and implies that $\langle (-W/Q_H)^n \rangle = \langle -W/Q_H \rangle^n = \left(1 - \frac{\omega_B}{\omega_A}\right)^n$, namely there are no efficiency fluctuations.

The simplest way to find explicitly the probability is to proceed from Eq. (31) by using the expression of the characteristic function in the last line of Eq. (B2), and one obtains

$$\begin{aligned} p[Q_H = n\omega_A] &= \int_0^{2\pi} \frac{d\mu}{2\pi} \left(\cos^2 \theta e^{-in\mu} + \sin^2 \theta \frac{1}{Z_A Z_B} \sum_{l,s=0}^{d-1} e^{-l\beta_A\omega_A} e^{-s\beta_B\omega_B} e^{i(l-s-n)\mu} \right) \\ &= \delta_{n,0} \cos^2 \theta + \sin^2 \theta \frac{1}{Z_A Z_B} \sum_{s=\max\{0,-n\}}^{d-1-\max\{0,n\}} e^{-s(\beta_A\omega_A + \beta_B\omega_B)} e^{-\beta_A\omega_A n}, \end{aligned} \quad (33)$$

which can be summarized as

$$p[Q_H = n\omega_A] = \delta_{n,0} \cos^2 \theta + \sin^2 \theta \frac{1}{Z_A Z_B} \frac{1 - e^{-(d-|n|)(\beta_A\omega_A + \beta_B\omega_B)}}{1 - e^{-(\beta_A\omega_A + \beta_B\omega_B)}} \times \begin{cases} e^{-\beta_A\omega_A n} & \text{for } 0 \leq n \leq d-1, \\ e^{-\beta_B\omega_B |n|} & \text{for } 1-d \leq n < 0. \end{cases} \quad (34)$$

In Fig. 6 we report the probability for the stochastic work in $(\omega_A - \omega_B)$ units for $\beta_A\omega_A = 1$ and $\beta_B\omega_B = 2$ and dimension $d = 8$, pertaining to three increasing values of the strength interaction, i.e. $\theta = \pi/4$, $\pi/3$, and $\pi/2$.

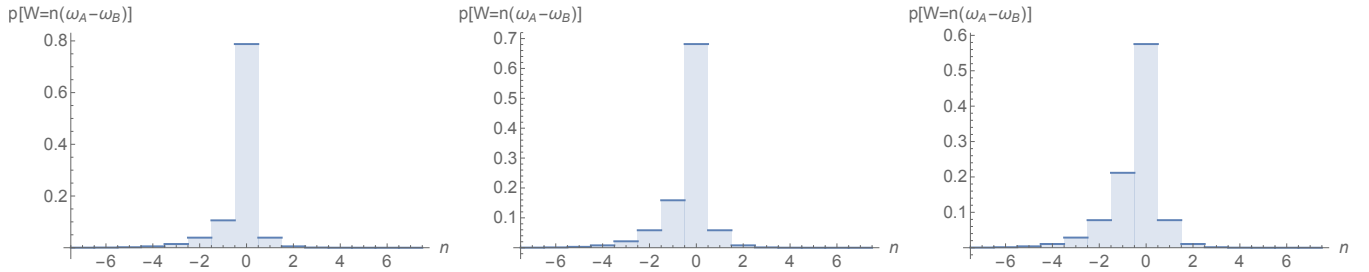


Figure 6. Probability of the stochastic work in $\omega_A - \omega_B$ units, for $\beta_A\omega_A = 1$ and $\beta_B\omega_B = 2$ and dimension $d = 8$, with strength interaction $\theta = \pi/4$ (left), $\pi/3$ (center), $\pi/2$ (right). By exchanging $n \rightarrow -n$, the same histograms represent the distribution of heat released by the hotter reservoir in ω_A units [see Eq. (32)].

The closed form for the probability in Eq. (34) allows one to explicitly verify the detailed fluctuation theorem in Eq. (11) as follows

$$\frac{p[W = -n(\omega_A - \omega_B), Q_H = n\omega_A]}{p[W = n(\omega_A - \omega_B), Q_H = -n\omega_A]} = e^{(\beta_B\omega_B - \beta_A\omega_A)n} = e^{(\beta_B - \beta_A)n\omega_A - \beta_B n(\omega_A - \omega_B)} = e^{(\beta_B - \beta_A)Q_H + \beta_B W}. \quad (35)$$

IV. FINITE-TIME ANALYSIS FOR PERFECT-SWAP STROKES

The thermal strokes considered in the previous sections implicitly assume infinite duration in order to guarantee a complete relaxation of the qudits by weak coupling to the temperatures of the respective thermal reservoirs. This means that indeed the output power per cycle becomes vanishing. However, the efficiency for a working cycle at finite times and hence with non-zero output power is usually of great practical importance [3, 61, 81–83, 88–90].

In this section we provide a preliminary study of the finite-time performance of the presented model for the specific case of perfect-swap operation $\theta = \pi/2$, postponing a general analysis for future work. In fact, as previously noticed after Eq. (23), a bi-thermal state of the qudits remains factorized and bi-thermal under perfect-swap operation. Then, we can provide a simple model for the effect of partial thermalization in the case of finite-time stroke, without resorting to a specific master-equation approach. After a number of transient cycles, the state of the two qudits will rapidly achieve the steady state of the map given by the composition of the swap stroke followed by the thermal stroke. Indeed, let us consider a time-dependent relaxation of the mean occupation number for both qudits towards their respective equilibrium values N_A and N_B as

$$\frac{dN_X(t)}{dt} = -\alpha_X [N_X(t) - N_X] \quad (36)$$

for $X = A, B$, where α_X denotes the relaxation rate constants and N_X are given by Eq. (15). Clearly, we have $N_X(t) = [N_X(0) - N_X]e^{-\alpha_X t} + N_X$. By taking thermal strokes with finite duration τ_q , at the end of the $(n+1)$ -th cycle the state will be bi-Gibbsian and the mean occupation numbers will satisfy the recursive relations

$$\begin{aligned} N_A^{(n+1)} &= (N_B^{(n)} - N_A)e^{-\alpha_A \tau_q} + N_A, \\ N_B^{(n+1)} &= (N_A^{(n)} - N_B)e^{-\alpha_B \tau_q} + N_B. \end{aligned} \quad (37)$$

The cycles lead to a periodic state corresponding to the steady-state solution given by

$$\begin{aligned} N_A^* &= \frac{N_A(1 - e^{-\alpha_A \tau_q}) + N_B(1 - e^{-\alpha_B \tau_q})e^{-\alpha_A \tau_q}}{1 - e^{-(\alpha_A + \alpha_B) \tau_q}}, \\ N_B^* &= \frac{N_B(1 - e^{-\alpha_B \tau_q}) + N_A(1 - e^{-\alpha_A \tau_q})e^{-\alpha_B \tau_q}}{1 - e^{-(\alpha_A + \alpha_B) \tau_q}}. \end{aligned} \quad (38)$$

From Eqs. (38) we also note the symmetry relation

$$N_A^* - N_B^* = \frac{(1 - e^{-\alpha_A \tau_q})(1 - e^{-\alpha_B \tau_q})}{1 - e^{-(\alpha_A + \alpha_B) \tau_q}} (N_A - N_B). \quad (39)$$

For finite-time thermalization strokes, after a transient, the characteristic function in the limit cycle is then still given by Eq. (10) by replacing β_X with the effective inverse temperatures $\beta_X^* = g^{-1}(N_X^*)/\omega_X$ in terms of the inverse of the function g given in Eq. (15). The average work in the steady cycles is then given by

$$\langle W \rangle = (\omega_B - \omega_A)(N_A^* - N_B^*), \quad (40)$$

and for Eq. (39) a simple scaling factor appears with respect to Eq. (16). Since the entropy production is ascribed to the temperature of the thermal baths one has

$$\langle \Sigma \rangle = (\beta_B \omega_B - \beta_A \omega_A)(N_A^* - N_B^*), \quad (41)$$

and so Eq. (13) still holds. The second moment in Eq. (19) and the joint probability of the stochastic work and heat in Eq. (34) are obtained by the replacement $(\beta_A, \beta_B) \rightarrow (\beta_A^*, \beta_B^*)$. Hence, the efficiency of the swap engine remains a non-fluctuating quantity even in the finite-time regime and is still given by $\eta = 1 - \frac{\omega_B}{\omega_A}$.

By neglecting the unitary stroke duration (e.g., we can take $\kappa \gg 1$ and $\tau_w \ll 1$, with $\theta = \kappa \tau_w$ as an odd multiple of $\pi/2$), the output power per cycle is given by

$$P = \langle -W \rangle / \tau_q = (\omega_A - \omega_B)(N_A^* - N_B^*) / \tau_q. \quad (42)$$

By assuming for simplicity equal relaxation rates $\alpha_A = \alpha_B = \alpha$ for the two reservoirs, one has

$$P = \frac{\tanh(\alpha \tau_q / 2)}{\tau_q} (\omega_A - \omega_B)(N_A - N_B), \quad (43)$$

which is trivially maximized versus τ_q for $\tau_q \rightarrow 0$, giving finite power $P = \frac{\alpha}{2}(\omega_A - \omega_B)(N_A - N_B)$. This means that the maximum power is achieved by a bang-bang approach with very short-term strokes. By dropping the condition

$\tau_w \ll 1$, notice that the optimal power will be smaller and obtained for a non-zero finite value of τ_q , as shown in Fig. 7. These considerations are analogous with the results of Ref. [61] pertaining to finite-time four-stroke Otto engines. Notice that the previous results about the efficiency at maximum work (see Fig. 2) apply at maximum output power as well, since the dependence on time in Eq. (43) is simply given by a factor and the efficiency is unchanged and independent of the cycle duration. We note that the possibility of surpassing the Curzon-Ahlborn efficiency has been recognized in a number of different scenarios [3, 67, 71, 88–93].

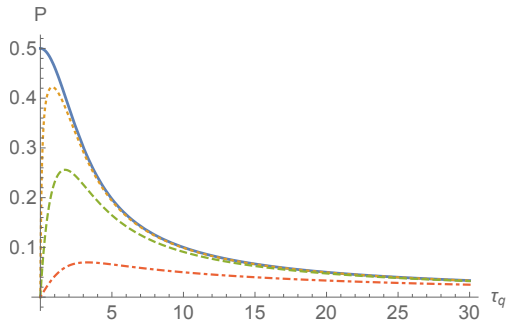


Figure 7. Power in $(\omega_A - \omega_B)(N_A - N_B)$ units versus thermalization stroke time τ_q with rates $\alpha_A = \alpha_B = 1$ and swap stroke times $\tau_w \rightarrow 0$ (solid line), $\tau_w = 0.1$ (dotted), $\tau_w = 1$ (dashed), and $\tau_w = 10$ (dot-dashed). In all cases, the condition $\kappa\tau_w = \pi/2$ is supposed to hold.

As in the two-mode bosonic Otto engine [60], short thermalization times are expected to be harmful for the signal-to-noise ratios of work and heat, with significant modification in the thermodynamic uncertainty relations. As an example, in Fig. 8 we plot the signal-to-noise ratio for fixed value of the parameter $N_B = 2$ versus varying N_A in the case of dimension $d = 9$, for different values of $\alpha\tau_q$, where it is apparent the detrimental effect of decreasing the thermalization times. These results can be obtained by replacing $f(\beta_A\omega_A, \beta_B\omega_B, d)$ with $f(\beta_A^*\omega_A, \beta_B^*\omega_B, d)$ in Eq. (22).

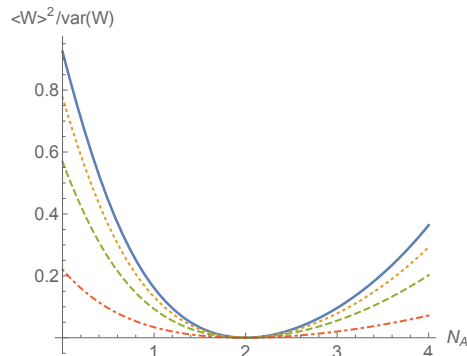


Figure 8. Signal-to-noise ratio of the work for a 9-level swap engine ($\theta = \frac{\pi}{2}$) with mean occupation number $N_B = 2$ versus varying N_A for ideal thermalization (solid), and finite thermalization stroke times $\alpha\tau_q = 3$ (dotted), 2 (dashed), and 1 (dot-dashed).

A deeper study of the finite-time scenario will be deferred for future work, possibly by the explicit modeling of the thermal relaxation via master equations and also by taking into account the residual correlations between the qudits in the steady state of the limit cycle in the case of partial-swap strokes.

V. CONCLUSIONS

By adopting the two-point-measurement scheme for the joint estimation of work and heat, we have quantified the work and heat fluctuations pertaining to two-qudit quantum thermodynamic two-stroke Otto engines, where the work is extracted or performed by a multilevel partial-swap interaction, and thermal relaxation to two respective reservoirs at different temperatures guarantees the cyclicity of the protocol. Exact relations among work, heat, fluctuations, efficiency, and reliability emerge.

We have derived the characteristic function for work and heat, and obtained the full joint distribution of the stochastic work and heat. In all ranges of coupling parameter and dimension we have shown thermodynamic uncertainty relations that reveal the interdependence among average extracted work, fluctuations and entropy production, confirming that reducing the noise-to-signal ratio of work or heat comes at a price of increased entropy production.

The link between fluctuation theorems and thermodynamic uncertainty relations appears to be relevant for the design of quantum thermodynamic machines. In fact, the presented results match the two-qubit swap engine with the two-mode bosonic case. In particular, we have shown that the small violation of the standard TUR for qubits is rapidly washed out for increasing dimension of the working qudits.

The effect of partial thermalization due to finite-time thermal strokes has also been studied in the case of perfect-swap unitary interaction. This results in a non-zero output power engine where the allocation of thermal and working strokes have been optimized. Thus, the efficiency at maximum power can be evaluated, and violations of the Curzon-Ahlborn limit are observed. Such violation are stronger for qubits and decrease for increasing dimension. We note, however, that partial thermalization sensibly decreases the signal-to-noise ratio of work and heat.

Appendix A: Derivation of the characteristic function $\chi(\lambda, \mu)$ in Eq. (9)

The characteristic function is given by the Fourier transform of the joint probability $p(W, Q_H)$ of the stochastic work W and heat Q_H , namely

$$\chi(\lambda, \mu) = \int dW \int dQ_H p(W, Q_H) e^{i\lambda W + i\mu Q_H}. \quad (\text{A1})$$

Let us adopt a two-point measurement protocol, where both the Hamiltonian H_A and H_B of the two isolated systems are measured just before and after the action of the unitary interaction $U(\tau_w)$. The probability $p_{n,m}$ for the initial measurement outcomes n and m is given by the Gibbs weight of the initial state ρ_0 , namely

$$p_{n,m} = \frac{1}{Z_A Z_B} e^{-\beta_A \omega_A n} e^{-\beta_B \omega_B m}. \quad (\text{A2})$$

The conditional probability $q(l, s|n, m)$ pertaining to the final measurement outcomes l and s given initial outcomes n and m is given by

$$q(l, s|n, m) = |\langle l| \otimes \langle s| U(\tau_w) |n\rangle \otimes |m\rangle|^2. \quad (\text{A3})$$

For this occurrence characterized by the set $\{n, m, l, s\}$ note that the work and heat are given by $\Delta E_A + \Delta E_B = \omega_A(l - n) + \omega_B(s - m)$ and $-\Delta E_A = \omega_A(n - l)$, respectively. Hence, the joint probability $p(W, Q_H)$ is obtained by the following average over all occurrences

$$p(W, Q_H) = \sum_{n,m,l,s} p_{n,m} q(l, s|n, m) \delta(W - \omega_A(l - n) - \omega_B(s - m)) \delta(Q_H - \omega_A(n - l)). \quad (\text{A4})$$

By replacing Eq. (A4) in (A1) and applying the delta functions one obtains

$$\begin{aligned} \chi(\lambda, \mu) &= \frac{1}{Z_A Z_B} \sum_{n,m,l,s} e^{-\beta_A \omega_A n} e^{-\beta_B \omega_B m} e^{i\lambda[\omega_A(l-n) + \omega_B(s-m)]} e^{i\mu \omega_A(n-l)} \\ &\quad \times \text{Tr}[U^\dagger(\tau_w)(|l\rangle\langle l| \otimes |s\rangle\langle s|)U(\tau_w)(|n\rangle\langle n| \otimes |m\rangle\langle m|)] \\ &= \text{Tr}[U^\dagger(\tau_w)(e^{i(\lambda-\mu)H_A} \otimes e^{i\lambda H_B})U(\tau_w)(e^{-i(\lambda-\mu)H_A} \otimes e^{-i\lambda H_B})\rho_0]. \end{aligned} \quad (\text{A5})$$

Appendix B: Evaluation of the characteristic function $\chi(\lambda, \mu)$ in Eq. (10)

For the unitary operator $U(\tau_w) = U_0(\tau_w)V_\theta$, since $U_0(\tau_w)$ commutes with both H_A and H_B , Eq. (10) rewrites as

$$\chi(\lambda, \mu) = \frac{1}{Z_A Z_B} \text{Tr}[V_\theta^\dagger(e^{i(\lambda-\mu)H_A} \otimes e^{i\lambda H_B})V_\theta(e^{-[i(\lambda-\mu)+\beta_A]H_A} \otimes e^{-(i\lambda+\beta_B)H_B})]. \quad (\text{B1})$$

Notice that the equivalence of the two expressions (10) and (B1) implies that by replacing the time-dependent interaction Hamiltonian in Eq. (3) with a constant quench Hamiltonian κE with strong parameter $\kappa \gg 1$ and short duration $\tau_w \ll 1$ with finite $\theta = \kappa \tau_w$ then one obtains the same statistics for the work and heat.

Since $V_\theta = \cos\theta I - i\sin\theta E$, from Eq. (B1) one has

$$\begin{aligned}\chi(\lambda, \mu) &= \cos^2\theta + \sin^2\theta \frac{1}{Z_A Z_B} \text{Tr}[E(e^{i(\lambda-\mu)H_A} \otimes e^{i\lambda H_B})E(e^{-[i(\lambda-\mu)+\beta_A]H_A} \otimes e^{-(i\lambda+\beta_B)H_B})] \\ &\quad + i\sin\theta \cos\theta \frac{1}{Z_A Z_B} \{ \text{Tr}[E(e^{i(\lambda-\mu)H_A} \otimes e^{i\lambda H_B})(e^{-[i(\lambda-\mu)+\beta_A]H_A} \otimes e^{-(i\lambda+\beta_B)H_B})] \\ &\quad - \text{Tr}[(e^{i(\lambda-\mu)H_A} \otimes e^{i\lambda H_B})E(e^{-[i(\lambda-\mu)+\beta_A]H_A} \otimes e^{-(i\lambda+\beta_B)H_B})] \} \\ &= \cos^2\theta + \sin^2\theta \frac{1}{Z_A Z_B} \text{Tr}[e^{(i\lambda \frac{\omega_B - \omega_A}{\omega_A} + i\mu - \beta_A)H_A} \otimes e^{-(i\lambda \frac{\omega_B - \omega_A}{\omega_B} + i\mu \frac{\omega_A}{\omega_B} + \beta_B)H_B}],\end{aligned}\quad (\text{B2})$$

where we used the identity $E(f(H_A) \otimes g(H_B))E = g(\omega_B H_A/\omega_A) \otimes f(\omega_A H_B/\omega_B)$ that holds for arbitrary functions f and g to simplify the factor of $\sin^2\theta$, and we applied the property $\text{Tr}[E(X \otimes Y)] = \text{Tr}[(X \otimes Y)E] = \text{Tr}[XY]$ for all operators X and Y to cancel out the two terms that multiply $\sin\theta \cos\theta$. Finally, by evaluating the trace we obtain

$$\begin{aligned}\chi(\lambda, \mu) &= \cos^2\theta + \sin^2\theta \frac{1}{Z_A Z_B} \frac{1 - e^{-d(\beta_A \omega_A + i\xi)}}{1 - e^{-(\beta_A \omega_A + i\xi)}} \frac{1 - e^{-d(\beta_B \omega_B - i\xi)}}{1 - e^{-(\beta_B \omega_B - i\xi)}} \\ &= \cos^2\theta + \sin^2\theta \frac{\sinh\left(\frac{\beta_A \omega_A}{2}\right) \sinh\left(\frac{\beta_B \omega_B}{2}\right) \sinh\left[\frac{d}{2}(\beta_A \omega_A + i\xi)\right] \sinh\left[\frac{d}{2}(\beta_B \omega_B - i\xi)\right]}{\sinh\left(\frac{d\beta_A \omega_A}{2}\right) \sinh\left(\frac{d\beta_B \omega_B}{2}\right) \sinh\left[\frac{1}{2}(\beta_A \omega_A + i\xi)\right] \sinh\left[\frac{1}{2}(\beta_B \omega_B - i\xi)\right]},\end{aligned}\quad (\text{B3})$$

where $\xi = (\omega_A - \omega_B)\lambda - \omega_A \mu$.

Appendix C: Efficiency at maximum work per cycle for $d \rightarrow \infty$

For $d \rightarrow \infty$ the maximum work per cycle is obtained from Eqs. (15) and (16) with $\theta = \pi/2$, and one has

$$|\langle W \rangle| = \frac{\omega_A - \omega_B}{2} \left[\coth\left(\frac{\beta_A \omega_A}{2}\right) - \coth\left(\frac{\beta_B \omega_B}{2}\right) \right]. \quad (\text{C1})$$

For fixed ratios $\eta_C = 1 - \frac{T_B}{T_A}$ and $\eta = 1 - \frac{\omega_B}{\omega_A}$ one can rewrite

$$|\langle W \rangle| = T_B \frac{\eta}{1 - \eta} x \left[\coth\left(\frac{1 - \eta_C}{1 - \eta} x\right) - \coth(x) \right], \quad (\text{C2})$$

with $x = \frac{\beta_B \omega_B}{2}$. Along similar lines as in Appendix D of Ref. [71] one easily shows that $|\langle W \rangle|$ achieves the maximum for $x \rightarrow 0$, since $\partial_x |\langle W \rangle| < 0$ for all $x > 0$. Hence, the maximum can be searched in the high-temperature limit [94], where

$$|\langle W \rangle| \simeq T_B \frac{\eta(\eta_C - \eta)}{(1 - \eta_C)(1 - \eta)} = T_B \left(1 - \frac{\omega_A}{\omega_B}\right) + T_A \left(1 - \frac{\omega_B}{\omega_A}\right), \quad (\text{C3})$$

which is maximized by the Curzon-Ahlborn value $\eta_m = \eta_{CA} = 1 - \sqrt{T_B/T_A}$.

-
- [1] N. Li, J. Ren, L. Wang, G. Zhang, P. Hänggi, and B. Li, Rev. Mod. Phys. **84**, 1045 (2012).
 - [2] G. Benenti, G. Casati, K. Saito, and R. S. Whitney, Phys. Rep. **694**, 1 (2017).
 - [3] F. Binder, L. A. Correa, C. Gogolin, J. Anders, and G. Adesso, eds., *Thermodynamics in the Quantum Regime* (Springer International Publishing, 2018).
 - [4] Y. Dubi and M. Di Ventra, Rev. Mod. Phys. **83**, 131 (2011).
 - [5] B. Rothmann, R. Sánchez, and A. N. Jordan, Nanotechnology **26**, 032001 (2015).
 - [6] F. Ritort, *Nonequilibrium Fluctuations in Small Systems: From Physics to Biology*, in Adv. Chem. Phys. **137**, 31 (2008).
 - [7] R. Rao and M. Esposito, Phys. Rev. X **6**, 041064 (2016).
 - [8] F. S. Gnesotto, F. Mura, J. Gladrow, and C. P. Broedersz, Rep. Prog. Phys. **81**, 066601 (2018).
 - [9] U. Seifert, Eur. Phys. J. B **64**, 423 (2008).
 - [10] M. Esposito, U. Harbola, and S. Mukamel, Rev. Mod. Phys. **81**, 1665 (2009).
 - [11] U. Seifert, Rep. Prog. Phys. **75**, 126001 (2012).
 - [12] D. J. Evans, E. G. D. Cohen, and G. P. Morriss, Phys. Rev. Lett. **71**, 2401 (1993).
 - [13] G. Gallavotti and E. G. D. Cohen, Phys. Rev. Lett. **74**, 2694 (1995).

- [14] C. Jarzynski, Phys. Rev. E **56**, 5018 (1997).
- [15] G. E. Crooks, J. Stat. Phys. **90**, 1481 (1998).
- [16] B. Piechocinska, Phys. Rev. A **61**, 062314 (2000).
- [17] C. Jarzynski and D. K. Wójcik, Phys. Rev. Lett. **92**, 230602 (2004).
- [18] U. Seifert, Phys. Rev. Lett. **95**, 040602 (2005).
- [19] U. M. B. Marconi, A. Puglisi, L. Rondoni, and A. Vulpiani, Phys. Rep. **461**, 111 (2008).
- [20] K. Saito and Y. Utsumi, Phys. Rev. B **78**, 115429 (2008).
- [21] P. Talkner, M. Campisi, and P. Hänggi, J. Stat. Mech. P02025 (2009).
- [22] D. Andrieux, P. Gaspard, T. Monnai, and S. Tasaki, New J. Phys. **11**, 043014 (2009).
- [23] M. Esposito and C. Van den Broeck, Phys. Rev. Lett. **104**, 090601 (2010).
- [24] M. Campisi, P. Talkner, and P. Hänggi, Phys. Rev. Lett. **105**, 140601 (2010).
- [25] N. A. Sinitsyn, J. Phys. A **44**, 405001 (2011).
- [26] M. Campisi, P. Hänggi, and P. Talkner, Rev. Mod. Phys. **83**, 771 (2011).
- [27] M. Campisi, J. Phys. A **47** 245001, (2014).
- [28] P. Hänggi and P. Talkner, Nat. Phys. **11**, 108 (2015).
- [29] R. Rao and M. Esposito, Entropy **20**, 635 (2018).
- [30] A. C. Barato and U. Seifert, Phys. Rev. Lett. **114**, 158101 (2015).
- [31] P. Pietzonka, A. C. Barato, and U. Seifert, Phys. Rev. E **93**, 052145 (2016).
- [32] T. R. Gingrich, J. M. Horowitz, N. Perunov, and J. L. England, Phys. Rev. Lett. **116**, 120601 (2016).
- [33] M. Polettini, A. Lazarescu, and M. Esposito, Phys. Rev. E **94**, 052104 (2016).
- [34] P. Pietzonka, F. Ritort, and U. Seifert, Phys. Rev. E **96**, 012101 (2017).
- [35] J. M. Horowitz and T. R. Gingrich, Phys. Rev. E **96**, 020103(R) (2017).
- [36] K. Proesmans and C. Van den Broeck, Europhys. Lett. **119**, 20001 (2017).
- [37] B. K. Agarwalla and D. Segal, Phys. Rev. B **98**, 155438 (2018).
- [38] T. Koyuk, U. Seifert, and P. Pietzonka, J. Phys. A **52**, 02LT02 (2018).
- [39] A. C. Barato, R. Chetrite, A. Faggionato, and D. Gabrielli, New J. Phys. **20**, 103023 (2018).
- [40] K. Brandner, T. Hanazato, and K. Saito, Phys. Rev. Lett. **120**, 090601 (2018).
- [41] P. Pietzonka and U. Seifert, Phys. Rev. Lett. **120**, 190602 (2018).
- [42] V. Holubec and A. Ryabov, Phys. Rev. Lett. **121**, 120601 (2018).
- [43] K. Macieszczak, K. Brandner, and J. P. Garrahan, Phys. Rev. Lett. **121**, 130601 (2018).
- [44] J. Li, J. M. Horowitz, T. R. Gingrich, and N. Fakhri, Nat. Commun. **10**, 1666 (2019).
- [45] S. Saryal, H. M. Friedman, D. Segal, and B. K. Agarwalla, Phys. Rev. E **100**, 042101 (2019).
- [46] A. Dechant, J. Phys. A **52**, 035001 (2019).
- [47] K. Proesmans and J. M. Horowitz, J. Stat. Mech. Theor. Exp. **2019**, 054005 (2019).
- [48] A. C. Barato, R. Chetrite, A. Faggionato, and D. Gabrielli, J. Stat. Mech. Theor. Exp. **2019**, 084017 (2019).
- [49] G. Guarnieri, G. T. Landi, S. R. Clark, and J. Goold, Phys. Rev. Res. **1**, 033021 (2019).
- [50] J. M. Horowitz and T. R. Gingrich, Nature Physics **16**, 15 (2020).
- [51] T. Van Vu and Y. Hasegawa, Phys. Rev. E **100**, 012134 (2019).
- [52] P. P. Potts and P. Samuelsson, Phys. Rev. E **100**, 052137 (2019).
- [53] A. M. Timpanaro, G. Guarnieri, J. Goold, and G. T. Landi, Phys. Rev. Lett. **123**, 090604 (2019).
- [54] Y. Hasegawa and T. Van Vu, Phys. Rev. Lett. **123**, 110602 (2019).
- [55] Y. Zhang, arXiv:1910.12862 (2019).
- [56] T. Van Vu and Y. Hasegawa, J. Phys. A **53**, 075001 (2020).
- [57] N. Merhav and Y. Kafri, J. Stat. Mech. Theor. Exp. **2010**, P12022 (2010).
- [58] H. Vroylandt, K. Proesmans, and T. R. Gingrich, J. Stat. Phys. **178**, 1039 (2020).
- [59] D. S. P. Salazar, Phys. Rev. E **103**, 022122 (2021).
- [60] M. F. Sacchi, Phys. Rev. E **103**, 012111 (2021).
- [61] T. Feldmann, E. Geva, R. Kosloff, and P. Salamon, Am. J. Phys. **64**, 485 (1996).
- [62] T. D. Kieu, Phys. Rev. Lett. **93**, 140403 (2004).
- [63] Y. Rezek and R. Kosloff, New J. Phys. **8**, 83 (2006).
- [64] H. T. Quan, Y.-x. Liu, C. P. Sun, and F. Nori, Phys. Rev. E **76**, 031105 (2007).
- [65] G. Thomas and R. S. Johal, Phys. Rev. E **83**, 031135 (2011).
- [66] O. Abah, J. Roßnagel, G. Jacob, S. Deffner, F. Schmidt-Kaler, K. Singer, and E. Lutz, Phys. Rev. Lett. **109**, 203006 (2012).
- [67] M. Campisi, J. P. Pekola, and R. Fazio, New J. Phys. **17**, 035012 (2015).
- [68] G. De Chiara, G. Landi, A. Hewgill, B. Reid, A. Ferraro, A. J. Roncaglia, and M. Antezza, New J. Phys. **20**, 113024 (2018).
- [69] J. P. S. Peterson, T. B. Batalhão, M. Herrera, A. M. Souza, R. S. Sarthour, I. S. Oliveira, and R. M. Serra, Phys. Rev. Lett. **123**, 240601 (2019).
- [70] O. A. D. Molitor and G. T. Landi, Phys. Rev. A **102**, 042217 (2020).
- [71] N. Piccione, G. De Chiara, and B. Bellomo, Phys. Rev. A **103**, 032211 (2021).
- [72] M. Saffman, T. G. Walker, and K. Molmer, Rev. Mod. Phys. **82**, 2313 (2010).
- [73] B. Yan, S. A. Moses, B. Gadway, J. P. Covey, K. R. A. Hazzard, A. M. Rey, D. S. Jin, and J. Ye, Nature **501**, 521 (2013).
- [74] C. Senko, P. Richerme, J. Smith, A. Lee, I. Cohen, A. Retzker, and C. Monroe, Phys. Rev. X **5**, 021026 (2015).

- [75] I. A. Silva, B. Çakmak, G. Karpat, E. L. G. Vidoto, D. O. Soares-Pinto, E. R. deAzevedo, F. F. Fanchini, and Z. Gedik, *Sci. Rep.* **5**, 14671 (2015).
- [76] V. Parigi, V. D'Ambrosio, C. Arnold, L. Marrucci, F. Sciarrino, and J. Laurat, *Nat. Comm.* **6**, 7706 (2015).
- [77] D.-S. Ding, W. Zhang, S. Shi, Z.-Y. Zhou, Y. Li, B.-S. Shi, and G.-C. Guo, *Light: Science & Applications* **5**, e16157 (2016).
- [78] M. Erhard, M. Krenn, and A. Zeilinger, *Nature Rev. Phys.* **2**, 365 (2020).
- [79] W. De Roeck and C. Maes, *Phys. Rev. E* **69**, 026115 (2004).
- [80] P. Talkner and P. Hänggi, *J. Phys. A* **40**, F569 (2007).
- [81] F. L. Curzon and B. Ahlborn, *Am. J. Phys.* **43**, 22 (1975).
- [82] B. Andresen, P. Salamon, and R. S. Berry, *J. Chem. Phys.* **66**, 1571 (1977).
- [83] J. Chen, *J. Phys. D: Appl. Phys.* **27**, 1144 (1994).
- [84] C. Jarzynski, *Phys. Rev. Lett.* **78**, 2690 (1997).
- [85] This can be easily inspected from Eq. (10), since the replacements $\lambda \rightarrow i\beta_B - \lambda$ and $\mu \rightarrow i(\beta_B - \beta_A) - \mu$ are equivalent to $\beta_A\omega_A + i\xi \leftrightarrow \beta_B\omega_B - i\xi$.
- [86] This can be explicitly seen by comparing the expression for the characteristic function $\chi(\lambda, \mu)$ in Eq. (B1) with Eq. (6) of Ref. [60] when in both equations one takes $\theta = \pi/2$.
- [87] A. Rignon-Bret, G. Guarnieri, J. Goold, and M. T. Mitchison, *Phys. Rev. E* **103**, 012133 (2021).
- [88] C. Van den Broeck, *Phys. Rev. Lett.* **95**, 190602 (2005).
- [89] M. Esposito, R. Kawai, K. Lindenberg, and C. Van den Broeck, *Phys. Rev. Lett.* **105**, 150603 (2010).
- [90] S. Deffner, *Entropy* **20**, 875 (2018).
- [91] P. P. Hofer, J.-R. Souquet, and A. A. Clerk, *Phys. Rev. B* **93**, 041418(R) (2016).
- [92] P. A. Erdman, V. Cavina, R. Fazio, F. Taddei, and V. Giovannetti, *New J. Phys.* **21**, 103049 (2019).
- [93] M. L. Bera, S. Julià-Farré, M. Lewenstein, and M. N. Bera, arXiv:2106.01193.
- [94] See also Eqs. (41) and (42) in Ref. [63].